Synthesis of Green Algal-Based Biochar for Remediation of Arsenic from Contaminated Waters

Ilyas Hussein Osman,[a] Syed Muhammad Usman Shah,[a,*] Nazneen Bangash,[a] Asia Nosheen,[a] Ismat Nawaz,[a] Syed Zafar Ilyas,[b] Nadir Zaman Khan,[c,*] Nawal H. Siddig,[d] Nawal Al-Hoshani,[e] Wejdan T. Alsaggaf,[f] Tariq Aziz, [g] Mohammed A. Alshehri, [h]

Arsenic (As) contamination of freshwater poses a major global public-health challenge. This study evaluated locally isolated freshwater green macroalgae as a feedstock for producing low-cost biochar for As(III) removal from aqueous solutions. Four filamentous chlorophytes, *Basicladia kosterae*, *Stigeoclonium tenue*, *Cladophora dalmatica*, and *Spirogyra fluviatalis*, were isolated from the Korang River (Islamabad, Pakistan), cultivated in BG11 medium, and combined in equal proportions to form a composite feedstock. The biomass was pyrolyzed at 500 °C under an N_2 atmosphere to produce composite algal biochar. FTIR analysis revealed O–H, C=O, and aromatic C–H functional groups that may contribute to arsenic adsorption, while XRF analysis indicated a high Fe content (~33 wt%), suggesting a role of Fe-(hydr)oxide phases in arsenic immobilization. Batch adsorption experiments were conducted at a biochar dosage of 10 g L^{-1} using initial As(III) concentrations of 0.05 to 0.5 ppm and contact times of 12 to 72 h. The highest removal efficiency (88 ± 3.5%) was achieved at 0.5 ppm after 12 h. These findings demonstrate the potential of indigenous freshwater algal biochar as an economical adsorbent for arsenic remediation. Further studies involving BET characterization, arsenic speciation, pH effects, post-adsorption analyses, and column-scale testing are needed to clarify adsorption mechanisms and practical applicability.

DOI: 10.15376/biores.21.3.7620-7639

Keywords: Freshwater macroalgae; Chlorophyta; Arsenic remediation; Algal biochar; Slow pyrolysis; FTIR; XRF; Surface complexation; Adsorption

Contact information: a: Department of Biosciences, COMSATS University Islamabad, Park Road, 44000, Islamabad, Pakistan; b: Department of Physics, Allama Iqbal Open University, Islamabad, Pakistan; c: Department of Biotechnology University of Malakand Chakdara Dir Lower KPK Pakistan; d: Department of Mathematical Science, College of Science, Princess Nourah bint Abdulrahman University, P.O. Box 84428, Riyadh 11671, Saudi Arabia; e: Department of Biology, College of Science , Princess Nourah bint Abdulrahman University, P.O. Box 84428, Riyadh 11671, Saudi Arabia; f: Chemistry Department, Faculty of Science, King Abdulaziz University, P.O. Box 80203, Jeddah 21589, Saudi Arabia; g: Biodiversity Genomics Unit, Faculty of Science, University of Tabuk, 71491, Tabuk, Saudi Arabia; h: Department of Biology, College of Science, University of Tabuk, 71491, Tabuk, Saudi Arabia;
** Corresponding authors: usman.kazmi@comsats.edu.pk; nadir.zaman@uom.edu.pk*

INTRODUCTION

Algae are the most abundant and diverse community of photosynthetic organisms that are similar to plants. Algae appear in various sizes and forms, ranging from unicellular to multicellular. Macroalgae and microalgae are two types of algae. Macroalgae, also

known as seaweed, are a type of multicellular alga usually found in the littoral, sublittoral, and intertidal regions (Hamed *et al*. 2018). Macroalgae is a renewable resource and abundant biomass that could be produced worldwide every year. They could also grow in water that is unsafe for drinking and do not need fertile agricultural land, so they can grow easily (Mobin and Alam 2017). Macroalgae are available everywhere around the world and have large economic benefits (Yang *et al*. 2015; Ghadiryanfar *et al*. 2016). Macroalgae have been used for bioremediation to extract contaminants from both natural and anthropogenic sources, and they have a lot of potential for treating heavy metal and nitrogen-polluted water (De Oliveira *et al*. 2016).

There is a rising interest in aquatic biomass, such as microalgae and macroalgae, particularly in those regions with extensive water surfaces. The attributes of the expected bioenergy material, which make them promising, include: the energy density, growth rate, photosynthesis rate, rate of CO_2 sequestration, oil content, adaptability, potential regarding the mitigation of greenhouse gas emissions, and absence of competition with agricultural land, all of which are higher in this material (Xu *et al*. 2019; Yuan *et al*. 2019). However, due to the lower concentration of cell biomass and cell size of microalgae, the use of macroalgae is more common (Hu *et al*. 2013).

Freshwater macroalgae represent an attractive feedstock for biochar production because they grow rapidly on non-arable land using poor-quality or contaminated water and do not compete with food production. Their polysaccharide-rich biomass and naturally accumulated mineral ions contribute oxygen-, nitrogen-, and metal-containing functional groups to the resulting biochar, which may enhance adsorption performance. In contrast to lignocellulosic woody biomass, freshwater filamentous algae possess higher native mineral content and provide additional in-stream bioremediation benefits through nutrient and heavy-metal uptake during growth. Importantly, the algal strains used in the present study are indigenous freshwater macroalgae without established high-value commercial applications; therefore, their conversion into biochar does not displace other economic uses. Furthermore, the energy demand of moderate-temperature slow pyrolysis (~500 °C) can be partially compensated by syngas and bio-oil co-products generated during the process. These combined factors provide a practical technical and economic rationale for utilizing freshwater macroalgae as a biochar precursor for arsenic remediation (Roberts *et al*. 2015; Raheem *et al*. 2018). On the basis of the foregoing, lignocellulosic and macroalgae biomass materials have been preferred for the production of biochar and co-pyrolysis. Heavy metals are commonly present in large amounts in wastewater. Due to their various metal sequestering features and potential to significantly reduce heavy metal ion concentration in solution, fresh and marine water algae are well-known natural biosorbents. In contrast to other physiochemical approaches such as ion exchange and chemical synthesis, the technique is recognized as environmentally friendly, cost-effective, reliable, and safe (Jaishankar *et al*. 2014; Bilal *et al*. 2018).

In many parts of the world, groundwater is the primary source of drinking water, particularly in developing countries like Bangladesh, Cambodia, India, Pakistan, China, Taiwan, Thailand, and Nepal (Hubadillah *et al*. 2020). Pakistan, as a developing nation, has been facing a serious shortage of clean and safe water supply in both urban and rural areas (Khan *et al*. 2015). The presence of arsenic (As) in subsurface aquifers and drinking water sources in some parts of Pakistan poses a significant human health threat (Malik *et al*. 2009). In Multan, Rahim Yar Khan, and Bahawalpur (Punjab), higher As concentrations of around 50 mg/L have been detected in drinking water, while in some areas of Sindh, such concentrations have risen four fold as compared to Punjab (Rasool *et al*. 2016). In

Pakistan, insufficient wastewater treatment and pollution from farm run-offs, industrial effluents, and urban wastewater are the major sources of As contamination (Ehsan *et al*. 2020). Many small-scale As removal technologies for use in communities and households have been developed, field-tested, and used under the action in many parts of the world over the last few years (Ahmed 2008). Furthermore, commercially available As removal technologies include adsorption, electro dialysis, chemical precipitation, membrane separation, and bioremediation through green algal biochar. The algal biochar derived from the remediation of wastewater can give a prominent advantage in the future by utilizing biomass for carbon negative energy generation and application to the environment (Yu *et al*. 2017).

Biochar is made by pyrolyzing low affordable biomass under oxygen-limited requirements. Biochar has a wide surface area, porous structure, and numerous functional groups, and so may be useful for the removal of various contaminants from aqueous solutions. In this context, biochar has received a lot of attention due to its inexpensive cost and efficiency at removing pollutants from water. The major benefits of bioremediation by these biosorbents for water pollution control include lower initial and operating costs, simple design, fast operation, and marginal toxic material effects (Deniz and Ersanli 2018).

Several key points provide important context for the adsorption of arsenic onto biochar. First, the dominant arsenic species in polluted waters are present as oxyanions: As(V) primarily exists as $H_2AsO_4^-$ and $HAsO_4^{2-}$ in the near-neutral pH range, whereas As(III) exists predominantly as the uncharged H_3AsO_3 species ($pKa_1 \approx 9.2$), with deprotonation occurring only at alkaline pH (Smedley and Kinniburgh 2002; Mohan and Pittman 2007). This negative or neutral character distinguishes arsenic adsorption from that of conventional heavy-metal cations and dictates fundamentally different binding mechanisms, such as inner-sphere ligand exchange on Fe- and Mn-(hydr)oxide surfaces, rather than electrostatic attraction (Wang and Mulligan 2006; Mohan and Pittman 2007). Second, the Brunauer-Emmett-Teller (BET) surface area of pristine biochar produced from biomass at moderate pyrolysis temperatures (400 to 600 °C, without chemical activation) is typically modest, generally in the range of 5 to 300 $m^2\ g^{-1}$ (Ahmad *et al.* 2014; Tan *et al.* 2015). In contrast, commercially produced activated carbons commonly exhibit surface areas of 600 to 1500 $m^2\ g^{-1}$ or higher, and can be specifically engineered through tailored chemical activation and impregnation with metal oxides (*e.g.*, Fe, Mn, Al, La) to provide high affinity for arsenic oxyanions (Mohan and Pittman 2007; Ali 2012). The present work therefore explores the inherent potential of unactivated freshwater algal biochar as a low-cost, environmentally derived adsorbent for arsenic, while acknowledging that future development through targeted activation or metal-impregnation strategies will likely be required to achieve performance comparable to engineered activated carbons.

Wastewater treatment from heterotrophic cultivation system applications used in algae processing is a fascinating premise for environmental cleaning (Adeniyi *et al*. 2018). Wood, agricultural leftovers, dairy manure, sewage sludge, and organic waste have been turned into biochars (Mohan *et al*. 2014). Biochar is a sustainable substance with great soil amendment, water remediation, and pollutant immobilisation performance. Biochar generated from macroalgae is a viable, low-cost alternative adsorbent since it is plentiful and has a high binding affinity for contaminants (Kim *et al*. 2016). It can adsorb organic and inorganic pollutants from polluted water. Biochar may improve food security through enhancing production processes, reduce Green House Gases emissions through carbon sequestration. The improvement in food production through biochar application in the soil have sparked worldwide interest in using biomass for sustainable energy generation and

eco-friendly environments (Kambo and Dutta 2015). Biochar on the soil may reduce sewage sludge or other pollution (Qambrani *et al*. 2017). In this regard, this work prepares biochar from freshwater macroalgae, determines its properties, and estimates arsenic absorption from synthetic waste water.

EXPERIMENTAL

Sample Collection and Culturing

The research work was performed in the biotechnology and applied microbiology laboratory, Department of Biosciences at COMSATS, University Islamabad Pakistan. Fresh water samples were collected from four sites (A, B, C, and D) of Korang River, Islamabad, Pakistan. Korang River is the outlet stream of Rawal Dam, located at 33° North latitude and 73° East longitude. Water temperature was recorded at each sampling site to characterize the environmental conditions affecting algal growth and distribution and to support the selection of laboratory cultivation conditions. The recorded temperatures were 20 °C for sample A, 22 °C for sample B, 24 °C for sample C, and 21 °C for sample D. The laboratory cultivation temperature of 25 to 30 °C was selected because it is widely reported as optimal for freshwater green macroalgae (Chlorophyta). Although the *in-situ* river temperatures were slightly lower, the selected cultivation range remained within the physiological tolerance of the isolates and promoted higher biomass accumulation for downstream pyrolysis. Algal samples were collected separately from each sampling site. Although each site contained 3 to 4 algal species, only the dominant species from each site was selected for further study. A unialgal strain from each site was subsequently isolated by repeated streaking on BG11 agar plates followed by serial sub-culturing under sterile conditions, resulting in a total of four isolates.

BG-11 medium was prepared using standard stock solutions of macronutrients and micronutrients. Macronutrient stock solutions included $MgSO_4 \cdot 7H_2O$ (75 g L^{-1}), $CaCl_2 \cdot 2H_2O$ (36 g L^{-1}), $C_6H_8O_7$ (6 g L^{-1}), Na_2EDTA (1 g L^{-1}), Na_2CO_3 (20 g L^{-1}), and $NaNO_3$ (150 g L^{-1}). For medium preparation, 1 mL of each macronutrient stock solution was added to ~400 mL of distilled water. The trace element solution consisted of H_3BO_3 (2.86 g L^{-1}), $MnCl_2 \cdot 4H_2O$ (1.81 g L^{-1}), $ZnSO_4 \cdot 7H_2O$ (0.222 g L^{-1}), $Na_2MoO_4 \cdot 2H_2O$ (0.39 g L^{-1}), $CuSO_4 \cdot 5H_2O$ (0.079 g L^{-1}), and $Co(NO_3)_2 \cdot 6H_2O$ (0.0494 g L^{-1}), prepared in 1 L distilled water. Subsequently, 1 mL of trace element solution was added to the medium. $C_6H_8FeNO_7$ (6 g L^{-1}) and K_2HPO_4 (40 g L^{-1}) were prepared separately and sterilized by autoclaving at 120 °C for 20 min along with the basal medium. After cooling to room temperature, sterile $C_6H_8FeNO_7$ and K_2HPO_4 were added aseptically under a biosafety cabinet, and the final volume was adjusted to 1 L with sterile distilled water. The optical density of cultures was also measured. A growth curve was created by measuring the OD values of cultures at 620 nm. Unless stated otherwise, the standard conditions for culture were 25 to 30 °C temperature, 24 h illumination, initial pH 7 to 7.5, and 90 µmol.photons m^2s^{-1} light intensity.

Morphological Identification

Botanical approaches were used for morphological identification. The morphological identification of macroalgae cultures was carried out in nutrient medium (Yang *et al*. 2021). The species were first isolated before being examined under a light microscope (40X, 60X and 100X). The isolated strains were compared with culture

collection of algae, University of Texas Austin (UTEX). Species-level identification was carried out based on detailed morphological characteristics and comparison with UTEX Culture Collection reference images. Diagnostic traits, including filament architecture, cell dimensions, chloroplast morphology and branching pattern closely matched UTEX references, supporting reliable preliminary species-level identification. Further confirmation using molecular markers such as 18S rRNA, rbcL, or ITS sequencing can be employed to validate species-level identity with higher taxonomic resolution.

Biomass Preparation and Pyrolysis

The freshwater green algae collected were washed extensively in the lab using deionized water. The algae was first sun dried for one week, and after 60% drying it was placed in electric oven for complete drying for 3 to 4 days. Each of the four isolates (tentatively identified as *B. kosterae*, *S. tenue*, *C. dalmatica*, and *S. fluviatalis*) was cultivated and dried separately. A representative composite feedstock was then prepared by combining equal dry-mass portions of all four species (1:1:1:1, w/w) prior to grinding. The equal-mass blending approach was selected to reflect the co-occurring riverine community, avoid single-species bias and represent a practically relevant scenario for field-scale bioremediation. The combined dry biomass was ground using a high-speed laboratory mill and sieved through a 60-mesh (≤250 µm) screen to ensure uniform particle size and improved heat transfer during pyrolysis. Pyrolysis of the composite feedstock was conducted in an electrically heated quartz-tube furnace. Approximately 15 g of the sieved biomass was placed in a quartz boat and introduced into the furnace. Prior to optimization, thermal screening was performed in the range of 300 to 700 °C, and the final pyrolysis conditions were set to a heating rate of 10 °C min^{-1} from room temperature to 500 °C, with a holding time of 60 min (total process time ≈ 3 h). A continuous flow of high-purity nitrogen gas (N_2, ≥99.99%, 100 mL min^{-1}) was maintained throughout the heating, pyrolysis, and cooling stages to ensure an inert atmosphere and reproducible conditions. The selection of 500 °C was based on achieving a balance between preservation of oxygen-containing functional groups at lower temperatures and enhanced aromatic carbon formation at higher temperatures. After cooling to room temperature under nitrogen, the biochar yield was determined gravimetrically. The resulting biochar was gently ground, stored in sealed polypropylene containers, and kept in the dark at room temperature (Michalak *et al*. 2019).

Biosorption of Algal Biochar

Working As(III) solutions were prepared by dissolving arsenic trioxide (As_2O_3) in deionised water to obtain nominal concentrations of 0.05, 0.10, 0.30, and 0.50 ppm. Batch adsorption experiments were conducted by adding 0.5 g of composite algal biochar (10 g L^{-1}) into 100 mL polypropylene centrifuge tubes containing 50 mL of As(III) solution (headspace ~50 mL). The tubes were agitated on an orbital shaker at 150 rpm at 25 ± 2 °C in the dark, and the initial pH of the solutions was adjusted to 7.0 ± 0.2. Each concentration–time combination was performed in triplicate (n = 3). At predetermined contact times (12, 24, 48, and 72 h), samples were centrifuged at 3000 rpm for 10 min at 4 °C, and the supernatant was collected for residual arsenic analysis. The recovered biochar was rinsed with deionised water, oven-dried at 45 °C overnight, gently ground, and stored for further analysis. Removal efficiencies are reported as mean ± standard deviation (n = 3), and statistical significance was evaluated using one-way ANOVA followed by Tukey's post-hoc test ($p < 0.05$).

The results should be interpreted in light of a methodological limitation of the present study. As_2O_3 was dissolved in water hydrolyses to arsenous acid (H_3AsO_3), which is moderately soluble (~20 g L^{-1} at 25 °C) but remains predominantly in the uncharged, non-dissociated form across the entire pH range relevant to this study ($pKa_1 \approx 9.2$; Smedley and Kinniburgh 2002; Mohan and Pittman 2007). Under the experimental conditions (initial pH 7.0 ± 0.2, ambient temperature, sealed polypropylene tubes), the introduced As(III) was therefore expected to be predominantly present as the neutral H_3AsO_3 species. In natural systems, As(III) and As(V) can be interconverted by biological and abiotic redox processes depending on aeration, dissolved oxygen, and the presence of Fe and Mn (hydr)oxides (Sharma and Sohn 2009; Bissen and Frimmel 2003). However, in the present experiment, redox state was not controlled, oxidation-reduction potential (E_h) and dissolved O_2 were not monitored, and arsenic speciation in the supernatant was not measured. Consequently, the extent to which partial oxidation of As(III) to As(V) may have occurred during the 12 to 72 h contact period is not known. This is acknowledged as an important limitation of the current preliminary study. Speciation-resolved arsenic analysis (*e.g.*, HPLC-ICP-MS) and E_h/DO monitoring are recommended for follow-up work, and are discussed further in the "Future Work" section.

SEM, FTIR, and XRF Analysis

Scanning electron microscopy (SEM) was used to examine the surface morphology and porosity of the pristine (pre-adsorption) algal biochar using a Cube-II tabletop SEM equipped with an energy-dispersive X-ray spectrometer. Images were acquired at an accelerating voltage of 9 kV under low-vacuum conditions (10 to 270 Pa). Fourier-transform infrared (FTIR) spectroscopy was employed to identify surface functional groups potentially involved in arsenic binding, including O–H, C=O, C=C, C–H, and aromatic C–H groups. Prior to analysis, biochar samples were dried at 80 °C for 24 h and analyzed using a Bruker FTIR spectrometer (RT-DLaTGS ZnSe detector). X-ray fluorescence (XRF) analysis was performed to determine the inorganic elemental composition of the biochar, which is relevant to surface reactivity, pH buffering capacity, and potential contributions of mineral phases to arsenic immobilization. Measurements were conducted at 25 kV, 0.54 mA over an energy range of 0 to 40 keV.

RESULTS AND DISCUSSION

Morphological Identification

Light microscopic examination of the four purified isolates at 40×, 60×, and 100× magnifications revealed distinct morphological characteristics, including filament architecture, branching pattern, chloroplast morphology and cell dimensions, which enabled species-level identification through comparison with UTEX reference images (Wehr 2015). As shown in Fig. 1, the isolate obtained from site A exhibited morphological features consistent with *Basicladia kosterae* (Garbary 2010), while the isolate from site B closely resembled *Stigeoclonium tenue* (Mourão *et al.* 2020). Similarly, the isolate collected from site C showed diagnostic traits matching *Cladophora dalmatica* (Gestinari *et al*. 2010), whereas the isolate from site D corresponded closely to *Spirogyra fluviatalis* (Takano and Higuchi, 2019). The strong similarity between the original microscopic images and UTEX reference photographs supported reliable identification of the macroalgal isolates. However, further confirmation using molecular markers such as 18S

rRNA, rbcL, or ITS sequencing is recommended to achieve higher taxonomic resolution. The optical density of cultures was also measured. A growth curve was constructed by measuring the OD values of cultures at 620 nm after every 4th day.

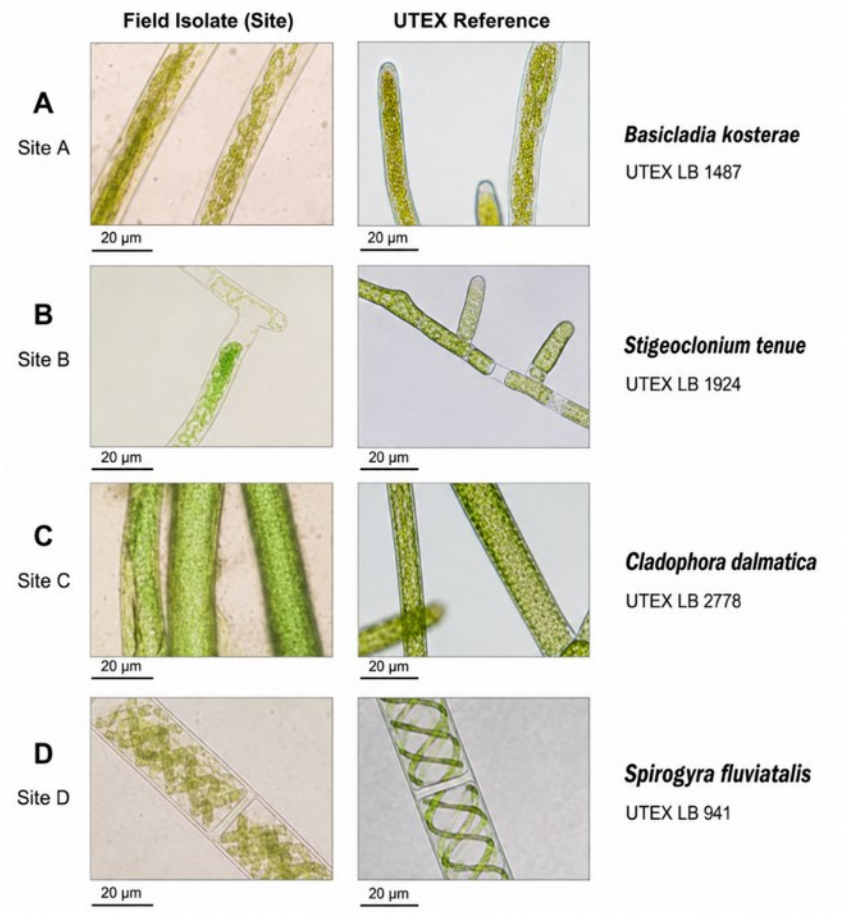

Fig. 1. Morphological comparison of algal isolates from sites A-D (left) with corresponding UTEX reference images (right) for species identification: (A) *Basicladia kosterae*, (B) *Stigeoclonium tenue*, (C) *Cladophora dalmatica*, and (D) *Spirogyra fluviatalis*

Growth Curves under Basic Culture Conditions

Figure 2 illustrates the biomass accumulation patterns of the four algal isolates under identical cultivation conditions. *Stigeoclonium tenue* showed comparatively lower biomass on Day 1, whereas *Spirogyra fluviatalis* exhibited the highest biomass on Day 5. By Days 9 and 13, *Spirogyra fluviatalis* and *Basicladia kosterae* produced the greatest biomass among the tested species. Since all isolates were cultivated under the same temperature, light, photoperiod, and nutrient conditions, the observed variations in biomass are attributed to intrinsic species-specific growth characteristics rather than environmental influences. The growth-curve analysis was primarily used to identify the late exponential to early stationary growth phase (Days 9 to 13) for optimal biomass harvesting prior to pyrolysis. Similar results have been reported for specific growth rate of *Neochloris conjuncta*, *Neochloris terrestris*, *Neochloris texensis*, *Botryococcus braunii*, and *Scenedesmus obliquus* (Krzemińska and Trzcińska 2014).

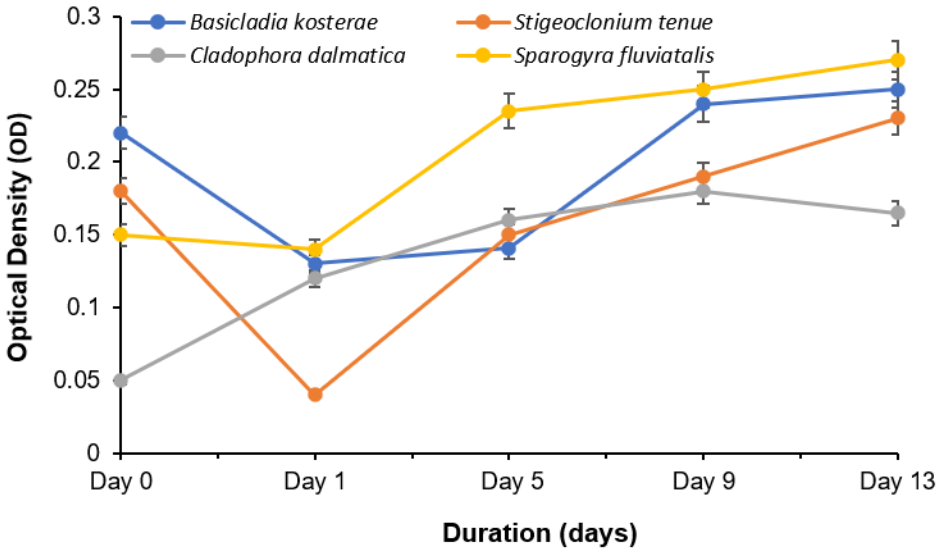

Fig. 2. Growth curves of four locally isolated freshwater green macroalgae (identified as *Basicladia kosterae*, *Stigeoclonium tenue*, *Cladophora dalmatica*, and *Spirogyra fluviatalis*) cultivated in BG11 medium under controlled conditions (25 to 30 °C, continuous illumination at 90 µmol photons m^{-2} s^{-1}, initial pH 7.0 to 7.5). Biomass accumulation was monitored *via* optical density at 620 nm and recorded at 4-day intervals.

Scanning Electron Microscopic Analysis of Algal Biochar

The surface morphology of the biochar was examined using scanning electron microscopy (SEM) at magnifications ranging from ×10,000 to ×20,000, with scale bars of 1.0 µm, 0.7 µm, and 0.5 µm (Fig. 3), using an accelerating voltage of 10 kV. The values 0.5 to 1.0 µm represent scale-bar lengths.

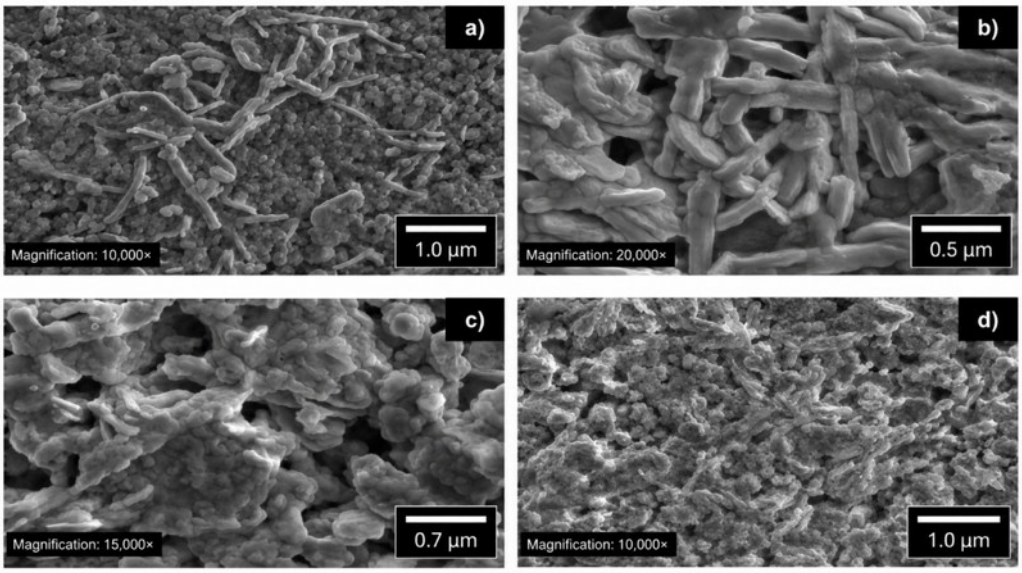

Fig. 3. Scanning electron microscopy (SEM) micrographs (a-d) of algal biochar showing a highly heterogeneous and porous surface morphology with irregular agglomeration, fibrous and layered structures, and abundant microcracks. Images were acquired at magnifications of ×10,000-×20,000 with scale bars of 1.0, 0.7, and 0.5 µm, revealing extensive surface roughness and pore development associated with pyrolytic transformation.

The SEM micrographs revealed a highly heterogeneous and porous surface morphology characterized by irregular particle aggregation, fibrous and layered structures, surface roughness, and the presence of microcracks. These features are attributed to structural collapse and volatile removal during pyrolysis, including dehydration and thermal decomposition of organic constituents. Such morphological characteristics increase the available surface area and may provide additional active binding sites, thereby enhancing the potential of the biochar for arsenic adsorption and immobilization. However, it should be emphasized that SEM analysis provides only qualitative surface information; therefore, quantitative surface area determination would require Brunauer-Emmett-Teller (BET) analysis. The physical structure of any biochar is one of the key properties related to its remediation effect and the surface area of the substrate can be increased by several thousand folds (Ma *et al*. 2016). It is obvious from the previous studies that SEM can produce different pictures revealing changing trends in the structure (Kim *et al*. 2012; Al-Wabel *et al*. 2013).

Surface Functional Groups

In present study the results from the Fourier transform infrared (FTIR) spectra reveal peaks within the range 3420 to 3400 cm^{-1}, indicating the presence of O-H bond stretches due to the presence of hydroxyl (-OH) group in alcohols, phenols, and organic acids functional groups (Fig. 4). The intensity of these peaks reduced as the pyrolysis temperature rose in the biochar samples. The surface functional groups found in the biochar are important in the adsorption mechanism found in the biochar. It must be emphasised, however, that the mechanisms commonly invoked for the adsorption of conventional heavy metals (*e.g*., Cu^{2+}, Pb^{2+}, Cd^{2+}, Zn^{2+}) namely electrostatic attraction to deprotonated -OH or $-COO^-$ groups and cation-exchange are not directly transferable to arsenic. As(V) species ($H_2AsO_4^-$, $HAsO_4^{2-}$) carry a negative charge in the neutral pH range and would therefore experience electrostatic repulsion rather than attraction from anionic carbon surface groups; uncharged As(III) (H_3AsO_3) has no electrostatic driving force at all. The most plausible mechanisms for arsenic binding on the present biochar are therefore inner-sphere ligand-exchange complexation on Fe- and Mn-(hydr)oxide phases within the biochar, consistent with the high Fe content detected by XRF, and hydrogen bonding along with weak surface complexation involving the uncharged O–H, C=O, and aromatic groups identified by FTIR, rather than simple electrostatic attraction (Wang and Mulligan 2006; Mohan and Pittman 2007; Vithanage *et al.* 2017). The cation-exchange-style discussion is retained only as comparative background from the heavy-metal literature and should not be interpreted as describing the actual binding pathway for arsenic in this study. The general adsorption-mechanism framework proposed for divalent heavy metals on biochar by Deng *et al.* (2017) provides a useful conceptual basis for interpreting metal-biochar interactions. However, because As(III) exists predominantly as the neutral H_3AsO_3 species at near-neutral pH, this framework cannot be directly applied to arsenic adsorption, which is more likely governed by ligand exchange with Fe-(hydr)oxide phases and surface complexation rather than electrostatic interactions. It was reported by Zhang *et al*. (2015) that the elevated temperature of the pyrolysis process reduced the production of biochar and the contents of the acid functional groups such as carboxyl and hydroxyl, but elevated the production of the basic functional groups such as amine, pH, carbon stability, ash contents, and the yield of the gases. Some peaks appeared close to 2900 cm^{-1}. These were attributed to the stretched vibrations of the C-H bonds present in the aliphatic organic compounds (Godlewska and Michalak 2018). The peaks in the range 1400 to 1450 cm^{-1},

show C=C stretching. Similar peaks have been reported previously (Wang *et al*. 2018). The peaks in the range 1600 to 1700 cm^{-1} show the organic alcohols, phenols, ethers, esters, and C=O groups. Moreover, the peaks between 800 and 1000 cm^{-1}, out of plane aromatic C=H functional group was also recognized.

The hydrophilicity of biochar due to oxygen functional groups would enhance the mechanisms of adsorption in heavy metal ions elimination (Enaime and Lübken 2021). It is emphasised that this hydrophilicity-enhanced cation adsorption argument applies primarily to positively charged heavy-metal ions and not directly to arsenic oxyanions or to the uncharged H_3AsO_3 species present in the near-neutral pH range used here. In addition, the functional groups on biochar, including phenolic functional groups, are essential for the interactions of chemical bonds that are formed between the adsorbent and pollutant during adsorption (Nartey and Zhao 2014). It should be noted that the p*K*a of phenolic -OH groups is approximately 10 (Stumm and Morgan 1996); these groups therefore remain almost entirely protonated and uncharged under the near-neutral pH conditions of the present experiments and natural ambient waters. They are unlikely to drive substantial electrostatic interactions with the negatively charged As(V) oxyanions or with the neutral H_3AsO_3 species. Their plausible contribution to arsenic binding is therefore *via* hydrogen bonding or weak surface complexation, rather than *via* ion-exchange mechanisms typical of conventional cationic heavy metals. Additionally, it was noted that the surface functional group varied with pyrolysis temperature. These findings are consistent with earlier reported information based on *Gracilaria gracilis* and *Cladophora glomerata* isolated from Caspian Sea (Parsa and Abduli 2018). According to the FTIR data, the pyrolysis temperature and feedstock each have a considerable impact on the functional and chemical content of the biochar (Qambrani *et al*. 2017; Poo *et al*. 2018).

SEM analysis alone cannot substantiate the environmental applicability of the biochar for wastewater treatment. Therefore, the interpretation has been strengthened using complementary spectroscopic and elemental evidence. Mechanistically, the simultaneous presence of O–H (3420 to 3400 cm^{-1}), C=O/aromatic C=C (1600 to 1700 cm^{-1}), C–H (~2900 cm^{-1}), and out-of-plane aromatic C–H (800 to 1000 cm^{-1}) bands suggests that surface complexation *via* oxygen-containing functional groups (hydroxyl, carbonyl, and carboxyl) plays a dominant role in As binding. This is further supported by the high Fe content (Fe ~33 wt%) detected by XRF, indicating that Fe-(hydr)oxide phases formed during pyrolysis may also contribute to As(III)/As(V) immobilisation through inner-sphere complexation. The combined contributions of functional group-mediated surface complexation and Fe-assisted binding provide a mechanistic basis for the observed arsenic removal efficiency reported in the subsequent section, thereby supporting the environmental relevance of the biochar beyond morphological observations.

Elemental Composition of Algal Biochar

The inorganic elements (Fe, P, Mn, Zr, Pd, Ni, Zn, Au) were found from algal based biochar with different concentrations using XRF (Fig. 4). The Fe (33.43%) was highest in current algal biochar followed by P (13.54%), Mn (3.7%), Pd (2.5%), and Zr (2.46%) while a smaller amount of Pb (0.64%), Ni (0.98%), Zn (1.03%), and Au (2.22%) were also observed. A high amount of Fe demonstrates that it can act as an active phase and improve the surface reaction. The detection of Pd (~2.5 wt%) and Au (~2.22 wt%) is unlikely for freshwater algal biochar and is most probably due to XRF spectral overlap or matrix effects; therefore, these signals should be interpreted cautiously and verified by ICP-MS. The relatively high Fe content likely reflects bioaccumulation from source water

concentrated during pyrolysis and may enhance As(III)/As(V) immobilisation *via* inner-sphere complexation on in situ–formed Fe-(hydr)oxide phases.

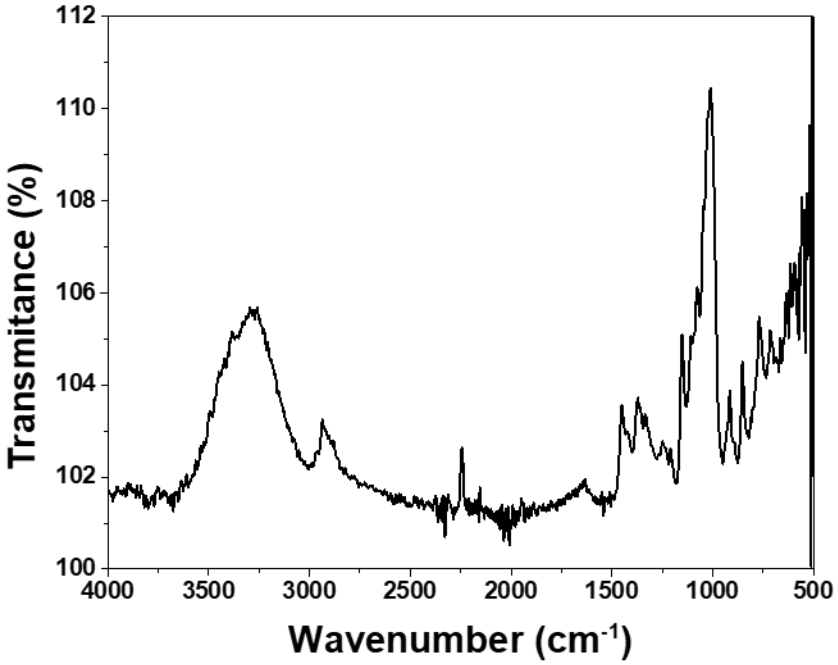

Fig. 4. FTIR spectra of composite freshwater algal biochar prepared from an equal-mass (1:1:1:1, w/w) blend of *Basicladia kosterae*, *Stigeoclonium tenue*, *Cladophora dalmatica*, and *Spirogyra fluviatalis*, produced *via* slow pyrolysis at 500 °C. Spectra were recorded using a Bruker Optik GmbH RT-DLaTGS ZnSe detector. Prior to analysis, samples were oven-dried at 80 °C for 24 h. Key diagnostic bands include O–H stretching (3420–3400 cm^{-1}), aliphatic C–H stretching (~2900 cm^{-1}), C=O/aromatic C=C vibrations (1600–1700 cm^{-1}), C=C bending (1400–1450 cm^{-1}), and out-of-plane aromatic C–H deformation (800–1000 cm^{-1})

Although Pb (~0.64 wt%) and Ni (~0.98 wt%) are minor relative to total biochar mass, their concentrations exceed established biochar quality limits for soil amendment (IBI/EBC guidelines). These metals are likely derived from environmental bioaccumulation and possible atmospheric contamination during processing. Accordingly, the produced biochar is unsuitable for soil application and is recommended only for adsorption-based wastewater treatment followed by safe disposal of spent material. Prior to any environmental application, standardized leaching (*e.g.,* TCLP or EN 12457-2) and risk assessment studies are required, along with evaluation of mitigation strategies such as feedstock pre-treatment, washing, or cultivation under controlled clean-water conditions. The algal biochar contains inorganic elements including Fe, P, Mn, Zr, Pd, Ni, Zn, and Au with different compositions. Metals including earth alkali and alkali metals found in the mineral composition of biochar would raise its pH and encourage the functional groups production in the biochar containing oxygen (Ronsse *et al*. 2013; Yu *et al*. 2017). Components of these minerals might aid in the adsorption of pollutants. Additionally, the inorganic salts might function as organic agents that form pores to give the biochar a structure that is hierarchically porous (Ho *et al*. 2019). Inorganic metals including K, Mg, Fe, and Ca present in some green seaweed showed fast and maximum removal efficiency in textile wastewater (Wang *et al*. 2020; Yuan *et al*. 2022). Freshwater macroalgal biochar is an effective and environmentally acceptable alternative to traditional adsorptive

materials. High level of Zn, Cu, and Cr removal was previously obtained from biochar of a freshwater macroalga *Cladophora* (Michalak *et al*. 2019).

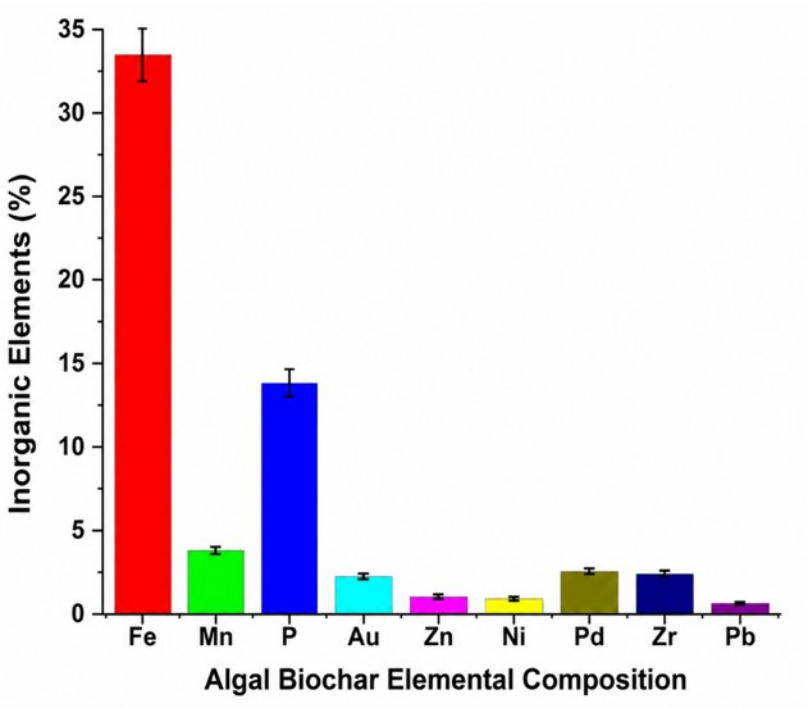

Fig. 5. Elemental composition (wt%) of composite freshwater algal biochar (1:1:1:1, w/w) produced at 500 °C under N_2 atmosphere and analyzed by XRF/ICP-OES (Agilent 5110). Apparent Pd and Au signals are considered probable XRF spectral overlap artefacts and require ICP-MS confirmation. Pb and Ni concentrations exceeded recommended IBI/EBC guideline values for soil-amendment biochars.

Arsenic Removal Efficiency of Macroalgal Biochar

The highest removal efficiency of algal biochar was observed at 0.5 ppm concentration of As when it was exposed for 12 and 24 h, and the lowest removal efficiency was observed at 0.05 ppm when it was exposed for 48 and 72 h. The highest removal efficiency was 88% and 84% while the lowest removal efficiency was 35% and 30%, respectively (Table 1 and Fig. 6). The adsorption behavior exhibited clear time- and concentration-dependent trends. An unexpected decrease in arsenic removal efficiency was observed with increasing contact time, particularly at lower initial arsenic concentrations. While adsorption typically increases until equilibrium is attained, decreases in apparent uptake have been reported when weakly bound adsorbates undergo partial desorption or when surface re-equilibration occurs during extended contact periods. In biochar systems, prolonged contact may alter surface functional groups, release dissolved organic constituents, or promote competitive interactions that reduce net adsorption (Mohan and Pittman 2007; Vithanage *et al*. 2017). In the present study, arsenic speciation and post-adsorption surface chemistry were not investigated; therefore, the precise mechanism responsible for the observed decline cannot be determined. Further studies involving arsenic speciation analysis, dissolved organic carbon measurements, and characterization of spent biochar are required to clarify the processes governing long-term arsenic retention. These results are in line with the reported 90.2% elimination of As utilizing the two macroalgal species *S. wightii* and *G. corticata* (Christobel and Lipton 2015). According to

a study, biochar might likely be used to treat wastewater during the bio-filtration stage. The effectiveness of biochar to lower the chemical parameters to the values recommended by Environmental Management Agent (EMA) has been reported by Manyuchi *et al*. (2018). Another study that combined post-hydrothermal liquefaction (HTL) and raw wastewater, the wastewater successfully investigated the effectiveness of a microalgal-based biochar at removing nutrients (Arun *et al*. 2020).

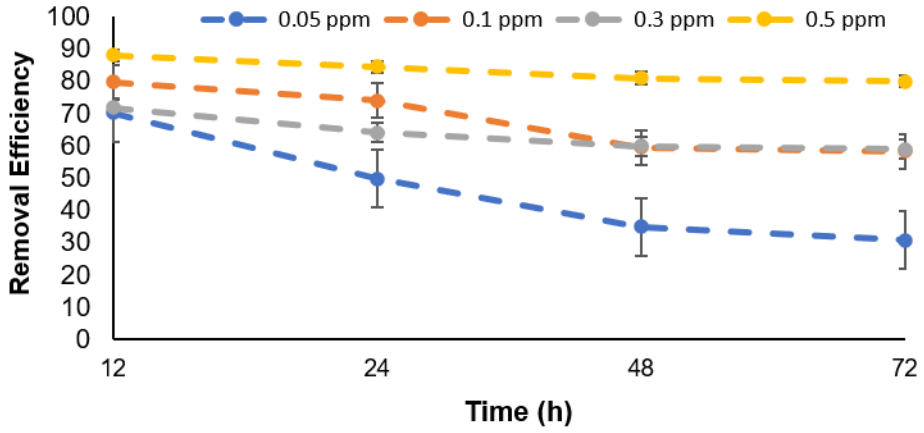

Fig. 6. Arsenic(III) removal efficiency of the composite freshwater algal biochar as a function of initial As concentration (0.05, 0.10, 0.30, and 0.50 ppm) and contact time (12, 24, 48, and 72 h). Experimental conditions: biochar dosage 10 g/L (0.5 g in 50 mL solution), 100 mL polypropylene centrifuge tubes, orbital shaking at 150 rpm, 25 ± 2 °C, initial pH 7.0 ± 0.2, in dark conditions. Data are presented as mean ± SD (n = 3). Note: the vertical-axis ordinate represents the fraction (in %) of arsenic removed from solution relative to the initial concentration, *i.e.* Removal efficiency (%) $= \frac{A_i - A_f}{A_i} \times 100.$

Table 1. Average As (III) Removal Efficiency (%) of Composite Freshwater Algal Biochar at Initial As(III) Concentrations (0.05-0.50 ppm) and Contact Times (12-72 h)

Conc. of As (ppm)	Average Removal efficiency (%) $= \frac{A_i - A_f}{A_i} \times 100$			
	12 Hrs	24 Hrs	48 Hrs	72 Hrs
0.05	70±0.76	50±1.23	35±0.82	31±1.36
0.1	80±2.16	74±0.63	60±1.72	58±2.55
0.3	72±2.33	64±3.18	60±1.45	59±2.16
0.5	88±3.45	85±1.46	81±2.27	80±3.44

The percentage of arsenic removed from solution relative to the initial concentration.

Future Work

The findings reported here should be regarded as preliminary, and additional investigations are required to further validate and extend the present work. Arsenic-speciation-resolved analyses (*e.g.*, HPLC-ICP-MS) of the supernatant before and after biochar contact are needed to determine whether As(III) is oxidized to As(V) during the adsorption process and to identify the species responsible for uptake. Simultaneous monitoring of dissolved oxygen, oxidation–reduction potential (E_h), and final pH would provide a clearer understanding of the system redox conditions. Quantitative characterization of the biochar by N_2 adsorption–desorption (BET) analysis is necessary to determine specific surface area and pore-size distribution and to facilitate comparison with other adsorbent materials. Adsorption experiments conducted across a range of pH values and in the presence of competing anions, including phosphate, silicate, sulfate, and bicarbonate, would help clarify the relative contributions of ligand exchange, surface complexation, and electrostatic interactions to arsenic removal. Evaluation under more realistic treatment conditions, including natural groundwater matrices, extended contact periods, and continuous-flow column operation, would provide information relevant to practical application. Comparative SEM-EDX and FTIR analyses of pristine and spent biochar, together with XPS characterization of arsenic-loaded materials, would offer direct evidence of adsorption mechanisms and arsenic speciation on the biochar surface. In addition, chemical activation approaches (KOH, H_3PO_4, and $ZnCl_2$) and metal impregnation strategies (Fe, Mn, Al, and La) should be investigated to enhance adsorption performance. Regeneration studies and standardized leaching assessments, such as TCLP and EN 12457-2, are also recommended to evaluate the long-term stability and environmental safety of the material.

CONCLUSIONS

1. Four freshwater green macroalgae from Korang River (sites A-D) were isolated as dominant unialgal strains and cultivated in BG11 medium, reaching late-exponential and early-stationary phase within Days 9 to 13 under uniform conditions.
2. Light microscopy (10×-100×) and UTEX comparison identified isolates as *Basicladia kosterae* (A), *Stigeoclonium tenue* (B), *Cladophora dalmatica* (C), and *Spirogyra fluviatalis* (D). This identification is morphology-based and requires molecular confirmation.
3. Composite algal biochar showed porous, fibrous morphology; XRF indicated Fe dominance (~33 wt%) with P, Mn, and Zr, suggesting As immobilization potential, while Pd and Au signals are likely artefacts requiring ICP-MS validation.
4. Fourier transform infrared (FTIR) spectra confirmed oxygen functional groups, and batch adsorption (10 g L^{-1}, 25 ± 2 °C, 150 rpm, n = 3) achieved 84 to 88% As(III) removal (0.5 ppm, 12 to 24 h), indicating strong adsorption with rapid initial uptake.
5. Elevated Pb and Ni levels restrict application to wastewater treatment only, with safe disposal of spent biochar. Further work is needed on BET surface area, leaching, regeneration, column studies and real-water testing before practical environmental deployment.

ACKNOWLEDGMENTS

The authors acknowledge the assistanceship to ILyas Hussein Osman and the research facilities by COMSATS University Islamabad. The authors are thankful to Princess Nourah bint Abdulrahman University Researchers Supporting Project number (PNURSP2026R924), Princess Nourah bint Abdulrahman University, Riyadh, Saudi Arabia.

Funding

This research was funded by Higher Education Commission Pakistan NRPU Grant Scheme (5390/Federal/NRPU/R&D/HEC/2016). The authors are thankful to Princess Nourah bint Abdulrahman University Researchers Supporting Project number (PNURSP2026R924), Princess Nourah bint Abdulrahman University, Riyadh, Saudi Arabia.

Competing Interests

The authors declare that there are no conflicts of interest.

Availability of Data and Material

All the data generated in this research work have been included in this manuscript.

REFERENCES CITED

Adeniyi, O. M., Azimov, U., and Burluka, A. (2018). "Algae biofuel: Current status and future applications," *Renewable and Sustainable Energy Reviews* 90, 316-335. https://doi.org/10.1016/j.rser.2018.03.067

Ahmad, M., Rajapaksha, A. U., Lim, J. E., Zhang, M., Bolan, N., Mohan, D., Vithanage, M., Lee, S. S., and Ok, Y. S. (2014). "Biochar as a sorbent for contaminant management in soil and water: A review," *Chemosphere* 99, 19-33. https://doi.org/10.1016/j.chemosphere.2013.10.071

Ahmed, M. F. (2008). "Water supply technologies for arsenic mitigation," In: *Arsenic Contamination of Groundwater: Mechanism, Analysis, and Remediation*, pp. 329-365. John Wiley and Sons, Inc. NJ. https://doi.org/10.1002/9780470371046

Ali, I. (2012). "New generation adsorbents for water treatment," *Chemical Reviews* 112(10), 5073-5091. https://doi.org/10.1021/cr300133d

Al-Wabel, M. I., Al-Omran, A., El-Naggar, A. H., Nadeem, M., and Usman, A. R. (2013). "Pyrolysis temperature induced changes in characteristics and chemical composition of biochar produced from conocarpus wastes," *Bioresource Technology* 131, 374-379. https://doi.org/10.1016/j.biortech.2012.12.165

Arun, J., Gopinath, K. P., Vigneshwar, S. S., and Swetha, A. (2020). "Sustainable and eco-friendly approach for phosphorus recovery from wastewater by hydrothermally carbonized microalgae: Study on spent bio-char as fertilizer," *Journal of Water Process Engineering* 38, article 101567. https://doi.org/10.1016/j.jwpe.2020.101567

Bilal, M., Rasheed, T., Sosa-Hernández, J. E., Raza, A., Nabeel, F., and Iqbal, H. (2018). "Biosorption: An interplay between marine algae and potentially toxic elements—a review," *Marine Drugs* 16(2), article 65. https://doi.org/10.3390/md16020065

Bissen, M., and Frimmel, F. H. (2003). "Arsenic – A review. Part I: Occurrence, toxicity, speciation, mobility," *Acta Hydrochimica et Hydrobiologica* 31(1), 9-18. https://doi.org/10.1002/aheh.200390025

Christobel, J., and Lipton, A. P. (2015). "Evaluation of macroalgal biomass for removal of heavy metal Arsenic (As) from aqueous solution," *International Journal of Application or Innovation in Engineering and Management* 4(5), 94-104.

De Oliveira, V. P., Martins, N. T., Guedes, P. D. S., Pollery, R. C. G., and Enrich-Prast, A. (2016). "Bioremediation of nitrogenous compounds from oilfield wastewater by *Ulva lactuca* (Chlorophyta)," *Bioremediation Journal* 20(1), 1-9. https://doi.org/10.1080/10889868.2015.1114463

Deng, H., Gao, R., Liao, X., and Cai, Y. (2017). "CRISPR system in filamentous fungi: current achievements and future directions," *Gene* 627, 212-221. https://doi.org/10.1016/j.gene.2017.06.019

Deniz, F., and Ersanli, E. T. (2018). "An ecofriendly approach for bioremediation of contaminated water environment: Potential contribution of a coastal seaweed community to environmental improvement," *International Journal of Phytoremediation* 20(3), 256-263. https://doi.org/10.1080/15226514.2017.1374335

Ehsan, N., Shan, A., Riaz, S., uz Zaman, Q., Javied, S., and Jabeen, M. (2020). "Health risk assessment due to exposure of arsenic contamination in drinking water of district Shiekhupura, Punjab, Pakistan," *Human and Ecological Risk Assessment: An International Journal* 26(1), 162-176. https://doi.org/10.1080/10807039.2018.1498292

Enaime, G., and Lübken, M. (2021). "Agricultural waste-based biochar for agronomic applications," *Applied Sciences* 11(19), article 8914. https://doi.org/10.3390/app11198914

Garbary, D. J. (2010). "Taxonomy of Basicladia (Cladophorales, Chlorophyta) with two new combinations," *Novon: A Journal for Botanical Nomenclature* 20(1), 38-40. https://doi.org/10.3417/2008020

Gestinari, L. M. D., Pereira, S. M. B., and Yoneshigue-Valentin, Y. (2010). "Distribution of Cladophora species (Cladophorales, Chlorophyta) along the Brazilian coast," *Phytotaxa* 14(1), 22-42. https://doi.org/10.11646/phytotaxa.14.1.2

Ghadiryanfar, M., Rosentrater, K. A., Keyhani, A., and Omid, M. (2016). "A review of macroalgae production, with potential applications in biofuels and bioenergy," *Renewable and Sustainable Energy Reviews* 54, 473-481. https://doi.org/10.1016/j.rser.2015.10.022

Godlewska, K., Marycz, K., and Michalak, I. (2018). "Freshwater green macroalgae as a biosorbent of Cr (III) ions," *Open Chemistry* 16(1), 689-701. https://doi.org/10.1515/chem-2018-0075

Hamed, S. M., Abd El-Rhman, A. A., Abdel-Raouf, N., and Ibraheem, I. B. (2018). "Role of marine macroalgae in plant protection & improvement for sustainable agriculture technology," *Beni-Suef University Journal of Basic and Applied Sciences* 7(1), 104-110. https://doi.org/10.1016/j.bjbas.2017.08.002

Ho, S. H., Li, R., Zhang, C., Ge, Y., Cao, G., Ma, M., ... and Ren, N. Q. (2019). "N-doped graphitic biochars from C-phycocyanin extracted *Spirulina* residue for catalytic persulfate activation toward nonradical disinfection and organic oxidation," *Water Research* 159, 77-86. https://doi.org/10.1016/j.watres.2019.05.008

Hu, H. Y., Liu, H., Shen, W. Q., Luo, G. Q., Li, A. J., Lu, Z. L., and Yao, H. (2013). "Comparison of CaO's effect on the fate of heavy metals during thermal treatment of

two typical types of MSWI fly ashes in China," *Chemosphere* 93(4), 590-596. https://doi.org/10.1016/j.chemosphere.2013.05.077

Hubadillah, S. K., Othman, M. H. D., Gani, P., Sunar, N. M., Tai, Z. S., Koo, K. N., ... and Zahari, S. S. N. S. (2020). "Integrated green membrane distillation-microalgae bioremediation for arsenic removal from Pengorak River Kuantan, Malaysia," *Chemical Engineering and Processing-Process Intensification* 153, article 107996. https://doi.org/10.1016/j.cep.2020.107996

Jaishankar, M., Tseten, T., Anbalagan, N., Mathew, B. B., and Beeregowda, K. N. (2014). "Toxicity, mechanism and health effects of some heavy metals," *Interdisciplinary Toxicology* 7(2), 60-72. https://doi.org/10.2478/intox-2014-0009

Kambo, H. S., and Dutta, A. (2015). "A comparative review of biochar and hydrochar in terms of production, physico-chemical properties and applications," *Renewable and Sustainable Energy Reviews* 45, 359-378. https://doi.org/10.1016/j.rser.2015.01.050

Khan, S., Shah, I. A., Muhammad, S., Malik, R. N., and Shah, M. T. (2015). "Arsenic and heavy metal concentrations in drinking water in Pakistan and risk assessment: A case study," *Human and Ecological Risk Assessment: An International Journal* 21(4), 1020-1031. https://doi.org/10.1080/10807039.2014.950925

Kim, H. S., Kim, K. R., Yang, J. E., Ok, Y. S., Owens, G., Nehls, T., ... and Kim, K. H. (2016). "Effect of biochar on reclaimed tidal land soil properties and maize (*Zea mays* L.) response," *Chemosphere* 142, 153-159. https://doi.org/10.1016/j.chemosphere.2015.06.041

Kim, K. H., Kim, J. Y., Cho, T. S., and Choi, J. W. (2012). "Influence of pyrolysis temperature on physicochemical properties of biochar obtained from the fast pyrolysis of pitch pine (*Pinus rigida*)," *Bioresource Technology* 118, 158-162. https://doi.org/10.1016/j.biortech.2012.04.094

Krzemińska, I., Pawlik-Skowrońska, B., Trzcińska, M., and Tys, J. (2014). "Influence of photoperiods on the growth rate and biomass productivity of green microalgae," *Bioprocess and Biosystems Engineering* 37(4), 735-741. https://doi.org/10.1007/s00449-013-1044-x

Ma, X., Zhou, B., Budai, A., Jeng, A., Hao, X., Wei, D., ... and Rasse, D. (2016). "Study of biochar properties by scanning electron microscope–energy dispersive X-ray spectroscopy (SEM-EDX)," *Communications in Soil Science and Plant Analysis* 47(5), 593-601. https://doi.org/10.1080/00103624.2016.1146742

Malik, A. H., Khan, Z. M., Mahmood, Q., Nasreen, S., and Bhatti, Z. A. (2009). "Perspectives of low cost arsenic remediation of drinking water in Pakistan and other countries," *Journal of Hazardous Materials* 168(1), 1-12. https://doi.org/10.1016/j.jhazmat.2009.02.031

Manyuchi, M. M., Mbohwa, C., and Muzenda, E. (2018). "Potential for treating sewage wastewater using sewage sludge biochar," *Covenant Journal of Physical & Life Sciences (CJPL)* 1(1), 1-7. https://repository.biust.ac.bw/handle/123456789/96

Michalak, I., Baśladyńska, S., Mokrzycki, J., and Rutkowski, P. (2019). "Biochar from a freshwater macroalga as a potential biosorbent for wastewater treatment," *Water* 11(7), article 1390. https://doi.org/10.3390/w11071390

Mobin, S., and Alam, F. (2017). "Some promising microalgal species for commercial applications: A review," *Energy Procedia* 110, 510-517. https://doi.org/10.1016/j.egypro.2017.03.177

Mohan, D. and Pittman, C.U. (2007). "Arsenic removal from water/wastewater using adsorbents—A critical review," *Journal of Hazardous Materials* 142(1), 1-53. https://doi.org/10.1016/j.jhazmat.2007.01.006

Mohan, D., Sarswat, A., Ok, Y. S., and Pittman Jr, C. U. (2014). "Organic and inorganic contaminants removal from water with biochar, a renewable, low cost and sustainable adsorbent–a critical review," *Bioresource Technology* 160, 191-202. https://doi.org/10.1016/j.biortech.2014.01.120

Mourão, M. M., Gradíssimo, D. G., Santos, A. V., Schneider, M. P. C., Faustino, S. M. M., Vasconcelos, V., and Xavier, L. P. (2020). "Optimization of polyhydroxybutyrate production by amazonian microalga *Stigeoclonium* sp. B23," *Biomolecules* 10(12), article 1628. https://doi.org/10.3390/biom10121628

Nartey, O. D., and Zhao, B. (2014). "Biochar preparation, characterization, and adsorptive capacity and its effect on bioavailability of contaminants: An overview," *Advances in Materials Science and Engineering* (1), 2014, article 715398. https://doi.org/10.1155/2014/715398

Parsa, M., Jalilzadeh, H., Pazoki, M., Ghasemzadeh, R., and Abduli, M. (2018). "Hydrothermal liquefaction of *Gracilaria gracilis* and *Cladophora glomerata* macro-algae for biocrude production," *Bioresource Technology* 250, 26-34. https://doi.org/10.1016/j.biortech.2017.10.059

Poo, K. M., Son, E. B., Chang, J. S., Ren, X., Choi, Y. J., and Chae, K. J. (2018). "Biochars derived from wasted marine macro-algae (*Saccharina japonica* and *Sargassum fusiforme*) and their potential for heavy metal removal in aqueous solution," *Journal of Environmental Management* 206, 364-372. https://doi.org/10.1016/j.jenvman.2017.10.056

Qambrani, N. A., Rahman, M. M., Won, S., Shim, S., and Ra, C. (2017). "Biochar properties and eco-friendly applications for climate change mitigation, waste management, and wastewater treatment: A review," *Renewable and Sustainable Energy Reviews* 79, 255-273. https://doi.org/10.1016/j.rser.2017.05.057

Raheem, A., Sikarwar, V. S., He, J., Dastyar, W., Dionysiou, D. D., Wang, W., and Zhao, M. (2018). "Opportunities and challenges in sustainable treatment and resource reuse of sewage sludge: A review," *Chemical Engineering Journal* 337, 616–641. https://doi.org/10.1016/j.cej.2017.12.149

Rasool, A., Farooqi, A., Masood, S., and Hussain, K. (2016). "Arsenic in groundwater and its health risk assessment in drinking water of Mailsi, Punjab, Pakistan," *Human and Ecological Risk Assessment: An International Journal* 22(1), 187-202. https://doi.org/10.1080/10807039.2015.1056295

Roberts, D. A., Paul, N. A., Cole, A. J., and de Nys, R. (2015). "From waste water treatment to land management: Conversion of aquatic biomass to biochar for soil amelioration and the fortification of crops with essential trace elements," *Journal of Environmental Management*, 157, 60-68. https://doi.org/10.1016/j.jenvman.2015.04.016

Ronsse, F., Van Hecke, S., Dickinson, D., and Prins, W. (2013). "Production and characterization of slow pyrolysis biochar: influence of feedstock type and pyrolysis conditions," *GCB Bioenergy* 5(2), 104-115. https://doi.org/10.1111/gcbb.12018

Sharma, V. K., and Sohn, M. (2009). "Aquatic arsenic: Toxicity, speciation, transformations, and remediation," *Environment International* 35(4), 743-759. https://doi.org/10.1016/j.envint.2009.01.005

Smedley, P.L. and Kinniburgh, D.G. (2002). "A review of the source, behavior, and distribution of arsenic in natural waters," *Applied Geochemistry* 17(5), 517-568. https://doi.org/10.1016/S0883-2927(02)00018-5

Stumm, W., and Morgan, J. J. (1996). *Aquatic Chemistry: Chemical Equilibria and Rates in Natural Waters*, 3rd Ed., John Wiley & Sons, New York, NY, USA.

Takano, T., Higuchi, S., Ikegaya, H., Matsuzaki, R., Kawachi, M., Takahashi, F., and Nozaki, H. (2019). "Identification of 13 *Spirogyra* species (Zygnemataceae) by traits of sexual reproduction induced under laboratory culture conditions," *Scientific Reports* 9(1), 1-11. https://doi.org/10.1038/s41598-019-43454-6

Tan, X., Liu, Y., Zeng, G., Wang, X., Hu, X., Gu, Y., and Yang, Z. (2015). "Application of biochar for the removal of pollutants from aqueous solutions," *Chemosphere* 125, 70-85. https://doi.org/10.1016/j.chemosphere.2014.12.058

Vithanage, M., Herath, I., Joseph, S., Bundschuh, J., Bolan, N., Ok, Y. S., Kirkham, M. B., and Rinklebe, J. (2017). "Interaction of arsenic with biochar in soil and water: A critical review," *Carbon* 113, 219-230. https://doi.org/10.1016/j.carbon.2016.11.032

Wang, S., and Mulligan, C. N. (2006). "Occurrence of arsenic contamination in Canada: Sources, behavior and distribution," *Science of the Total Environment* 366(2-3), 701-721. https://doi.org/10.1016/j.scitotenv.2005.09.005

Wang, S., Jiang, D., Cao, B., Qian, L., Hu, Y., Liu, L., Yuan, C., Abomohra, A. E., He, Z., Wang, Q., and Zhang, B. (2018). "Bio-char and bio-oil characteristics produced from the interaction of Enteromorpha clathrate volatiles and rice husk bio-char during co-pyrolysis in a sectional pyrolysis furnace: A complementary study," *Journal of Analytical and Applied Pyrolysis* 135, 219-230. https://doi.org/10.1016/j.jaap.2018.08.030

Wang, S., Zhao, S., Uzoejinwa, B. B., Zheng, A., Wang, Q., Huang, J., and Abomohra, A. E. F. (2020). "A state-of-the-art review on dual purpose seaweeds utilization for wastewater treatment and crude bio-oil production," *Energy Conversion and Management* 222, article 113253. https://doi.org/10.1016/j.enconman.2020.113253

Wehr, J. D. (2015). "Brown algae," in: *Freshwater Algae of North America*, Academic Press, pp. 851-871. https://doi.org/10.1016/B978-0-12-385876-4.00019-0

Xu, X., Wei, Z., Ji, Q., Wang, C., and Gao, G. (2019). "Global renewable energy development: Influencing factors, trend predictions and countermeasures," *Resources Policy* 63, article 101470. https://doi.org/10.1016/j.resourpol.2019.101470

Yang, Y., Chai, Z., Wang, Q., Chen, W., He, Z., and Jiang, S. (2015). "Cultivation of seaweed Gracilaria in Chinese coastal waters and its contribution to environmental improvements," *Algal Research* 9, 236-244. https://doi.org/10.1016/j.algal.2015.03.017

Yang, Y., Zhang, M., Alalawy, A. I., Almutairi, F. M., Al-Duais, M. A., Wang, J., and Salama, E. S. (2021). "Identification and characterization of marine seaweeds for biocompounds production," *Environmental Technology & Innovation* 24, article 101848. https://doi.org/10.1016/j.eti.2021.101848

Yu, K. L., Lau, B. F., Show, P. L., Ong, H. C., Ling, T. C., Chen, W. H., ... and Chang, J. S. (2017). "Recent developments on algal biochar production and characterization," *Bioresource Technology* 246, 2-11. https://doi.org/10.1016/j.biortech.2017.08.009

Yuan, C., Liu, Q., Wei, M., Zhao, S., Yang, X., Cao, B., Wang, S., Abomohra, A., Liu, X., and Hu, Y. (2022). "Selective oxidation of 5-hydroxymethylfurfural to furan-2, 5-dicarbaldehyde using chitosan-based biochar composite cadmium sulfide quantum dots," *Fuel* 320, article 123994. https://doi.org/10.1016/j.fuel.2022.123994

Yuan, X., He, P., Zhu, Q., and Li, X. (2019). "Adversarial examples: Attacks and defenses for deep learning," *IEEE Transactions on Neural Networks and Learning systems* 30(9), 2805-2824. https://doi.org/10.1109/TNNLS.2018.2886017

Zhang, J., Liu, J., and Liu, R. (2015). "Effects of pyrolysis temperature and heating time on biochar obtained from the pyrolysis of straw and lignosulfonate," *Bioresource Technology* 176, 288-291. https://doi.org/10.1016/j.biortech.2014.11.011

Article submitted: January 1, 2026; Peer review completed: April 23, 2026; Revised version received: June 4, 2026; Further revised version received: June 16, 2026; Accepted: June 17, 2026; Published: June 30, 2026.
DOI: 10.15376/biores.21.3.7620-7639